Interaction of Human Apolipoprotein A-I with Model Membranes Exhibiting Lipid Domains

Cristina Arnulphi,* Susana A. Sánchez,† M. Alejandra Tricerri,* Enrico Gratton,† and Ana Jonas*
*Department of Biochemistry, and †Laboratory for Fluorescence Dynamics, Department of Physics, University of Illinois at Urbana-Champaign, Champaign, Illinois

ABSTRACT Several mechanisms for cell cholesterol efflux have been proposed, including membrane microsolubilization, suggesting that the existence of specific domains could enhance the transfer of lipids to apolipoproteins. In this work isothermal titration calorimetry, circular dichroism spectroscopy, and two-photon microscopy are used to study the interaction of lipid-free apolipoprotein A-I (apoA-I) with small unilamellar vesicles (SUVs) of 1-palmitoyl, 2-oleoyl phosphatidylcholine (POPC) and sphingomyelin (SM), with and without cholesterol. Below 30°C the calorimetric results show that apoA-I interaction with POPC/SM SUVs produces an exothermic reaction, characterized as nonclassical hydrophobic binding. The heat capacity change (ΔC_p°) is small and positive, whereas it was larger and negative for pure POPC bilayers, in the absence of SM. Inclusion of cholesterol in the membranes induces changes in the observed thermodynamic pattern of binding and counteracts the formation of α-helices in the protein. Above 30°C the reactions are endothermic. Giant unilamellar vesicles (GUVs) of identical composition to the SUVs, and two-photon fluorescence microscopy techniques, were utilized to further characterize the interaction. Fluorescence imaging of the GUVs indicates coexistence of lipid domains under 30°C. Binding experiments and Laurdan generalized-polarization measurements suggest that there is no preferential binding of the labeled apoA-I to any particular domain. Changes in the content of α-helix, binding, and fluidity data are discussed in the framework of the thermodynamic parameters.

INTRODUCTION

Interaction of apolipoprotein A-I (apoA-I) or lipid-poor high-density lipoproteins (HDL) with the plasma membrane leads to the removal of cellular lipids. The metabolic events taking place in this process are a matter of debate. Plasma membrane proteins, such as the ATP Binding Cassette A1 (ABCA1), are well known to facilitate the efflux of phospholipids, mostly phosphatidylcholine (PC), toward nascent apolipoproteins that can then accept cholesterol (1). Cell lipid removal depends on factors including cell type and metabolic rate, as well as the nature of the acceptor of cell cholesterol (2). There has been an increasing interest in understanding the interaction of pure apolipoproteins with specific lipids due to the role that protein-lipid interactions play in defining the structure and function of apolipoproteins, and in modulating their metabolism (3–6). Different mechanisms for cell cholesterol efflux have been proposed, from unmediated aqueous diffusion to pathways involving specific apolipoprotein receptors expressed on the plasma membrane (7,8). It was suggested that the existence of specific domains could enhance the transfer of lipids to the apolipoproteins (7). Membrane microdomains enriched in sphingolipids and cholesterol (9) had been proposed to function in sorting and transporting lipids and proteins (10). These microdomains are recognized to exist within populations involved in cholesterol homeostasis, in the form of caveolae and lipid rafts (11,12). Probably due to their brief lifespan, it is not well known if they act as cholesterol donors for free cholesterol (Chol) efflux mediated by HDL. The possibility of lipid phase-separation in vivo, and the influence that lipid domains may have on the interaction with proteins have been intensively studied (13,14). With regard to apolipoprotein studies, Mendez et al. (15) examined whether ABCA1-mediated lipid efflux involves the selective removal of lipids associated with membrane rafts and concluded that the involvement of membrane rafts in cholesterol efflux applies to lipidated HDL particles but not to lipid-free apoA-I.

In this work, we examine apoA-I interaction with model membranes mimicking a putative lipid raft composition by using three different techniques: isothermal titration calorimetry (ITC), circular dichroism (CD) spectroscopy, and two-photon fluorescence microscopy. Microcalorimetry permits the accurate determination of association constants (K_a), stoichiometries of binding (n), and thermodynamics of binding (ΔH°, ΔG°). CD spectroscopy allowed us to determine the change in α-helical contents of apoA-I upon binding to the membranes. For these two techniques we have used small unilamellar vesicles as a lipid system. Two-photon microscopy allows the direct visualization of lipid systems, and the size of the giant unilamellar vesicles ($\approx$100 μm diameter) makes them very suitable for this purpose (16).

We have used this combination of techniques and systems in a previous study (17) on the interaction of apoA-I and 1-palmitoyl, 2-oleoyl phosphatidylcholine (POPC) vesicles (giant unilamellar vesicles and small unilamellar vesicles, i.e., GUVs and SUVs), showing that the lipid-free apolipoprotein

Submitted June 11, 2004, and accepted for publication April 7, 2005.

Address reprint requests to Dr. Cristina Arnulphi, Unidad de Biofísica, Universidad del País Vasco, PO Box 644, E-48080 Bilbao, Spain. Tel.: 34-94-601-3357; E-mail: arnulphi@hotmail.com.

0006-3495/05/07/285/11 $2.00

doi: 10.1529/biophysj.104.047480

was able to bind the vesicles but not able to form lipid-protein complexes. On the contrary, reconstituted HDL particles, especially the smaller complexes with 78 Å diameter, were efficient in binding to and removing lipids from the vesicles. In a more recent report we investigated, using ITC and CD spectroscopy, the interaction of apoA-I with model membranes made of pure POPC in the presence and absence of cholesterol (18). We found that the interaction of apoA-I with these vesicles followed a nonclassical hydrophobic interaction, driven by enthalpy rather than by entropy. The thermodynamic parameters showed that the membrane affinity of the protein increased with cholesterol, but the bilayer penetration of the protein as well as the number of bound protein molecules per vesicle decreased.

The present work is intended to explore the possible role of lipid domain separation in the interaction of apoA-I with POPC/sphingomyelin/Chol vesicles, on the basis of calorimetric, spectroscopic, and fluorescence microscopy data. The experimental results failed to reveal any preferential binding of apoA-I to specific domains. However, both sphingomyelin (SM) and Chol were found to affect in different ways the thermodynamics of apoA-I binding to lipid bilayers.

EXPERIMENTAL PROCEDURES

Materials

Human apoA-I was purified as described previously (19) from blood plasma purchased from the Champaign County Blood Bank of the Regional Health Center (Champaign, Illinois). 1-Palmitoyl-2-oleoyl phosphatidylcholine (POPC) and bovine brain sphingomyelin (SM) were purchased from Avanti Polar Lipids (Alabaster, AL); crystalline-free cholesterol (Chol) and Trizma HCl (Tris (hydroxymethyl) aminomethane hydrochloride) were from Sigma Biochemicals (St. Louis, MO); (^{3}H)-dipalmitoyl phosphatidylcholine (DPPC, 92.3 Ci/mmol) was from Du Pont-NEN (Boston, MA), and dichloromethane was from Fisher Scientific (Fairlawn, NJ). 6-Lauroyl-2-(dimethylamino) naphthalene (Laurdan) was purchased from Molecular Probes (Eugene, OR).

Methods

Small unilamellar vesicle (SUV) preparation

To prepare small unilamellar vesicles of 250–300 Å diameter, a given amount of POPC, with or without SM and Chol, was combined in CHCl3 with a trace amount of (^{3}H)-DPPC to a specific radioactivity of ~90 cpm/mg phospholipid. Lipids were dried under N2 at ~50°C and then redissolved in dichloromethane to remove trace amounts of chloroform; this is frequently used to stabilize CHCl3 (20). Samples were then dried again under a N2 stream at ~50°C before overnight drying under high vacuum. Dried lipids were dispersed in Tris salt buffer (TSB) containing 10 mM Tris HCl at pH 8.0, 0.15 M NaCl, 1 mM NaN_3, and 0.1 mM EDTA, and vortexed extensively to obtain a milky dispersion of multilamellar liposomes. The suspension was placed in an ice bath under a flow of N2, and sonicated at 35% amplitude using a 4-s on/4-s off pulse on a VCX-400 Vibra Cell with a microprobe (Sonics & Materials, Newtown, CT) until the solution became translucent. Titanium debris was removed by subsequent centrifugation for 10 min at 12,000 rpm. A homogeneous population of SUVs was purified from larger liposomes on a 1.5 × 60 cm Sepharose CL-4B column (Pharmacia Biotech, Uppsala, Sweden) equilibrated with TSB buffer. Radioactivity in the eluted fractions was detected and quantified by liquid scintillation counting. Typically, a small amount of larger liposomes was eluted in the excluded volume, and SUVs were eluted as a single symmetrical peak well separated from the larger liposome peak. The SUV fractions corresponding to half of the peak width were pooled and concentrated to ~4 mg/mL of phospholipid.

Isothermal titration microcalorimetry

Isothermal titration calorimetry was performed using the VP-ITC high sensitivity titration calorimeter (MicroCal, Northampton, MA); for further references see Wiseman (21). Typically, 20 consecutive 10 μL aliquots of the protein at a concentration of 30–100 μM were injected into the cell (1.43 mL) filled with 1–10 mM lipid solution. To minimize the contribution of dilution to the binding heat, both the protein solution and the SUV preparation were dialyzed against the same buffer before the ITC experiments. Both lipid and protein solutions were degassed under vacuum immediately before use. Injections were made at 10-min intervals and at 2 s/μL injected protein. A constant stirring speed of 300 rpm was maintained during the experiment to ensure proper mixing after each injection. Dilution heats of protein into the lipid solution were determined from the last few injections of the titration series, and subtracted from experimental heats of binding. These measured heats of dilution agreed with those obtained from the corresponding protein-buffer titration. Data were analyzed using the Origin software provided by MicroCal. For experiments where the reaction was fully exothermic, we were able to fit the experimental data to a Langmuir adsorption model of a single class of binding sites. Here binding means the adsorption of the protein from bulk solution to the lipid-buffer interface, and its partial insertion into the hydrophobic core of the bilayers. We cannot quantify the effects of cholesterol separately, so we refer to $PC \rightarrow SM$ interactions in the presence of Chol for implicitly taking into account Chol effects. The ITC protocol determines the molar enthalpy change ΔH of transfer of apoA-I from buffer into membranes. After each injection, a small aliquot of protein binds to the free vesicles in the cell, giving rise to measurable heat peaks. The integrated heats of injections are plotted versus protein concentration in the cell for experiments with PC/SM or PC/SM/Chol. At sufficiently large protein concentrations, virtually all apoA-I is bound and the process of binding comes to a halt. The affinity constant K_a of apoA-I for the membrane determines the number of protein molecules bound per lipid molecule (N), considering the whole lipid composition of the membrane (PC + SM or PC + SM + Chol).

The number of phospholipid molecules bound per apoA-I (r) was calculated from the N-values, by supposing that only 60% of the total lipids, located on the outer leaflet of the vesicles, are available for binding. Assuming that each vesicle contained 3000 phospholipid molecules (22), the number of apoA-I molecules bound per vesicle (n) can be estimated. An additional important parameter that could be obtained from calorimetric experiments, namely ΔH^o measurements as a function of T, is the heat capacity change per mol of protein (ΔC_p°). This parameter gives information about the nature of the forces responsible for the interaction (23–25). The equilibrium association constant (K_a), the enthalpy change (ΔH^o), and the stoichiometry parameter (N), were obtained from curve fitting of the experimental data to a Langmuir adsorption model of a single class of binding sites provided by Origin. The values obtained from the fitting were used to calculate the standard free energy change (ΔG^o) and the standard entropy change (ΔS^o) for the binding as dependent variables in the following equation where R is the molar gas constant:

$$\Delta G^o = -RT \ln K_a = \Delta H^o - T\Delta S. \quad (1)$$

Laurdan generalized polarization (GP) in SUVs

Laurdan emission maximum depends upon the phase state of the phospholipids, being blue in the gel (maximum emission ~440 nm), and green in the liquid crystalline phase (maximum ~490 nm). To quantify the

emission spectral changes, the generalized polarization function was defined as (26)

$$GP = I_B - I_R/I_B + I_R, \quad (2)$$

where I_B and I_R are the intensities in the blue and green edges of the emission spectrum. Thus, lower values of *GP* indicate an increased content or relaxation rate of water molecules surrounding Laurdan dipoles. SUVs were prepared as described previously, and Laurdan was added to a 1:100 probe/phospholipid molar ratio. Laurdan-doped vesicles were incubated at the desired temperatures, with or without protein, Laurdan emission spectrum was acquired with an excitation of 360 nm and emissions at 440 and 490 were registered and used to calculate *GP* (Eq. 2).

Preparation of giant unilamellar vesicles (GUVs)

Phospholipid stock solutions were prepared in chloroform at concentrations of 0.2 mg/mL. Two mixtures were used: POPC/SM (7.5:1.4 molar ratio) and POPC/SM/Chol (7.5:1.4:1.3 molar ratio). The electroformation method developed by Angelova and Dimitrov (27–29) was used to prepare the GUVs. The vesicles were formed in a temperature-controlled chamber that allows a working temperature range from 9°C to 80°C (16,30). Approximately 2 μl of the lipid stock solution were spread on the platinum (Pt) wire in the sample chamber under a stream of N_2. The chamber was subsequently lyophilized for ~1 h to remove any remaining traces of organic solvent. The chamber and the buffer (1 mM Tris, pH 8.0) were separately equilibrated to temperatures ≈10°C above the lipid mixture phase transition(s), then 4 mL buffer were added to cover the Pt wires. Immediately after buffer addition, the Pt wires were connected to a function generator (Hewlett-Packard, Santa Clara, CA), and a low-frequency AC field (sinusoidal wave function with a frequency of 10 Hz and amplitude of 2 V) was applied for 90 min. The AC field was turned off after GUVs were formed and the temperature was decreased slowly from the growing temperature (~60°C) to the desired temperature. The temperature was measured inside the chamber at the Pt wires, using a digital thermometer (Model 400B, Omega, Stamford, CT) with a precision of 0.1°C. A charge-coupled device video camera (CCD-Iris, Sony, San Diego, CA) was used to follow the formation of GUVs and to select the target vesicle. Laurdan was added to the sample chamber after the vesicles were formed to a final phospholipid/Laurdan molar ratio of ~100:1. Vesicles were homogeneously labeled with Laurdan within 15 min.

Two-photon microscopy of GUVs

To visualize the lateral organization of lipids, images from the surface of the Laurdan-doped GUVs were obtained in the two-photon fluorescence microscope designed at the Laboratory for Fluorescence Dynamics (31,32). This system has been extensively used for studying the phase behavior of artificial lipid mixtures, as well as natural lipid mixtures extracted from cell membranes (33,34). The visualization of coexisting domains was achieved by using two-photon excitation with polarized light as described before (33). An LD-Achroplan 20× long-working-distance air objective (Zeiss, Holmdale, NJ) with an N.A. of 0.4 was used. A titanium-sapphire laser (Mira 900; Coherent, Palo Alto, CA) pumped by a frequency-doubled Nd:Vanadate laser (Verdi; Coherent, Palo Alto, CA) set to 780 nm, was used as the excitation light source. A galvanometer-driven *x*,*y* scanner was positioned in the excitation path (Cambridge Technology Watertown, MA) to achieve beam scanning in both *x* and *y* directions. A frame rate of 9 s/frame was used in image acquisition (256 × 256 pixels). A quarter wave-plate (CVI Laser, Albuquerque, NM) was aligned and placed before the light entering the microscope to minimize polarization. The fluorescence emission was observed through a broad bandpass filter from 350 nm to 600 nm (BG39 filter; Chroma Technology, Brattleboro, VT). A miniature photomultiplier (R5600-P, Hamamatsu, Bridgewater, NJ) was used for light detection in the photon-counting mode. A commercial version (ISS card) of a card designed at the Laboratory for Fluorescence Dynamics (35) was used to acquire the counts.

ApoA-I binding to GUVs

ApoA-I was labeled with fluorescein as described previously (36). GUVs of POPC/SM with and without cholesterol at temperatures below 30°C were used. Labeled-apoA-I was added to a chamber with unlabeled GUVs as described before (17). A control scanning is taken before the protein is added into the chamber containing the vesicles. Once the image with the fluorescent protein was recorded, Prodan was added to identify the lipid domains (37).

*Laurdan generalized polarization (*GP*) and images*

In our two-photon microscope a dual-channel setup was used at the emission, and two simultaneous images were obtained, one for each region of the Laurdan spectra (33–38). The two images were analyzed by SimFCS (Laboratory for Fluorescence Dynamics, Champaign, IL) to obtain the *GP* image and the associated *GP* histogram (distribution of the *GP* values per pixel). To avoid deviations due to vesicle curvature, *GP* distributions were obtained at the center of the vesicle. When the GUV presents a homogeneous *GP* distribution, the *GP* histogram can be fitted to a single Gaussian distribution, where the value of *GP* at the center of the distribution corresponds to the average *GP* value. When two coexisting domains are observed in the GUV, the *GP* histogram shows two components and the average *GP* (GP_a) value is given by a sum of the fractional (*fr*) contribution of the pixels with different *GP*:

$$GP_a = GP_B fr_B + GP_G fr_G. \quad (3)$$

Circular dichroism spectroscopy

All CD measurements were carried out on JASCO-720 equipment (JASCO, Tokyo, Japan), at constant temperatures of 15°C or 37°C. In a typical experiment, 5 μl apoA-I at 2.15 mg/mL was incubated with 100 μl of POPC/SM or POPC/SM/Chol SUVs at 6.5 mg/mL. TSB buffer was added to a final volume of 200 μl. The samples were mixed and vortexed immediately before each experiment. The samples were placed in a 0.1-cm pathlength cuvette, and scanned from 250 to 190 nm with a 0.1-nm resolution using a 1.0-nm bandwidth. The fraction of α-helical structure ($f\Theta$) of apoA-I in solution and after incubation with lipid vesicles was estimated by using the empirical expression of Chen et al. (39),

$$f_\Theta = [\Theta]_{222} + 2340/(-30, 300), \quad (4)$$

where $[\Theta]_{222} = MRW \times \theta_{222}/10 \times l \times c$. Here θ_{222} is the negative ellipticity observed at 222 nm, l is the optical pathlength of the cuvette, c is the protein concentration, and MRW is the mean residue weight. An MRW of 115.4 was used for apoA-I of MW 28,000 Daltons.

RESULTS

Isothermal titration calorimetry

Binding of apoA-I to SUVs of phosphatidylcholine/sphingomyelin

The ITC experiments of apoA-I binding to lipid bilayers of phosphatidylcholine and sphingomyelin were carried out at several temperatures on samples of POPC/SM SUVs of 5.7:1.4 mol/mol. The titration yielded different responses depending on the temperature. When the titration was carried out above 30°C, the injections consistently produced positive peaks, corresponding to an endothermic process (Fig. 1 *A*). The pattern of the peaks could not be reproduced in separate

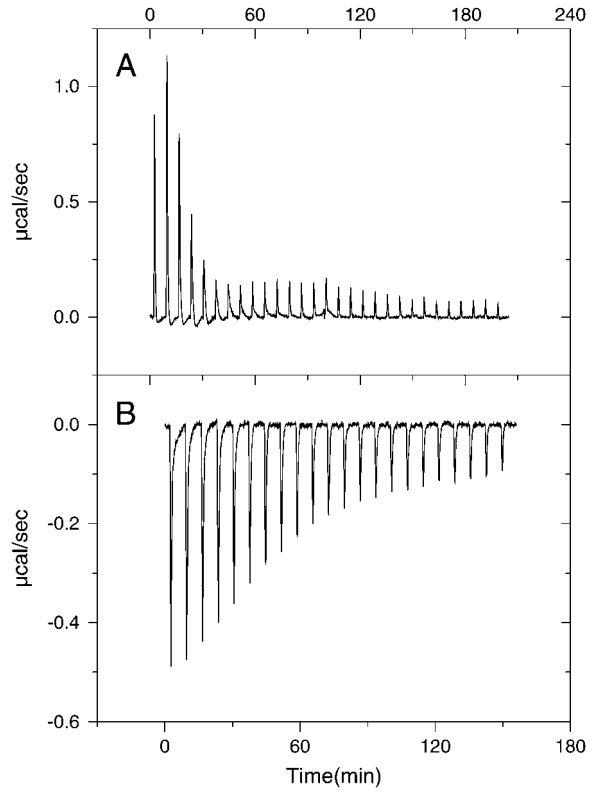

FIGURE 1 Thermograms obtained for the titration of apoA-I into POPC/SM SUVs (7.5:1.4 mol/mol ratio). Reactions were endothermic at 37°C (*A*) but exothermic at 15°C (*B*).

experiments, thus data were not suitable for fitting to any binding model. Between 15°C and 30°C, reactions were exothermic as indicated by the negative peaks of the thermogram (Fig. 1 *B*). The baseline was stable, and the signal returned to its initial value after a few minutes. The ITC data displayed in Table 1 are the average of parameters obtained in at least three separate experiments.

The equilibrium association constant (K_a) and the number of lipid molecules per bound apoA-I (r) were rather constant over the temperature range of 15–30°C. The mean values (between 3.6 and 4.7 $\times$ 10^6 M^{-1} for K_a and 1300 lipid molecules per protein), were very similar to those found for the binding of apoA-I to pure POPC SUVs (18).

For the binding reaction of apoA-I to POPC/SM vesicles, ΔH^o varied linearly with temperature, and a heat capacity change could be computed of $\Delta C_p^\circ = 0.81$ kcal/mol K. This unusual positive ΔC_p° was first observed for magainin binding to neutral bilayers (40). Those authors suggested that it would be the result of a perturbation of the lipid membrane so that hydrophobic surface areas became exposed to water. Additionally, because liquidlike hydrocarbon chains have a higher molar heat capacity than ordered chains, it could indicate that the interaction of the protein with the membrane induces disorder on the fatty acyl chain of the phospholipids. Positive ΔC_p° might also correspond to the transfer of some polar residues of apoA-I from the aqueous solution into the nonpolar environment of the membrane (41).

Binding of apoA-I to SUVs of phosphatidylcholine/sphingomyelin/cholesterol

To investigate the thermotropic binding behavior of apoA-I to a lipid raft model membrane, we prepared vesicles of POPC/SM/Chol (at a molar ratio of 7.5:1.4:1.3). This particular mixture mimicked the lipid composition of human platelet membranes (42). Recently, Almeida et al. (43) published the ternary phase diagrams of sphingomyelin/phosphatidylcholine/cholesterol, and discussed lipid rafts within the framework of liquid-ordered/liquid-disordered phase coexistence. According to their data, and under the experimental conditions used in our experiments, the bilayers to which apoA-I binds at 15°C have two coexisting fluid lipid phases: liquid-ordered (lo) and liquid-disordered (ld), the proportion of ld phase increasing with temperature, so that a homogeneous ld phase is observed at 30°C. This is further confirmed by fluorescence microscopy experiments described below.

It has been shown that membranes containing sufficient amounts of sphingolipid and sterol exhibit separation of discrete liquid-ordered (lo) and liquid-disordered (ld) phase domains (13). In addition, scanning calorimetric experiments with PC/SM/Chol and similar systems show a very broad peak that is often attributed to the transition from a liquid-ordered to a fluid state (44). In the present study, two different behaviors were observed depending on the temperature at which the experiments was performed. The titration peaks between 15 and 30°C were exothermic, and the corresponding isotherms fitted very well to a single binding site model. At temperatures higher than 30°C the first few injections produced exothermic peaks, although subsequent injections became endothermic. This behavior differs from the one observed for the interaction of apoA-I to membranes of POPC or to binary mixtures of POPC/Chol (18) or to POPC/SM shown here. The possible causes for this behavior will be discussed in

TABLE 1 Thermodynamic parameters (average of at least three experiments, ±SD) obtained by isothermal titration calorimetry for apoA-I binding to POPC/SM (molar ratio of 7.5:1.4) SUVs

T (°C)	N	r	n	K_a (M^{-1})	ΔH°_{prot} (kcal/mol)	ΔH°_{lipid}* (cal/mol)	$T\Delta S^\circ$ (kcal/mol)
15	$(4.6 \pm 0.4) \times 10^{-4}$	1295 ± 12	2.31	$(3.6 \pm 0.8) \times 10^6$	−38.9 ± 1.9	−30 ± 3	−30.5 ± 1.0
22	$(4.8 \pm 0.3) \times 10^{-4}$	1260 ± 88	2.38	$(4.7 \pm 0.2) \times 10^6$	−33.1 ± 1.5	−26 ± 2	−23.9 ± 1.2
30	$(4.6 \pm 0.3) \times 10^{-4}$	1304 ± 91	2.30	$(3.8 \pm 0.4) \times 10^6$	−26.7 ± 1.6	−20 ± 2	−17.6 ± 0.5

*$\Delta H^\circ_{lipid} = \Delta H^\circ_{prot}/r$.

the next section. Table 2 summarizes the values of the thermodynamic parameters measured for exothermic reactions, and Fig. 2 compares these values with that obtained for the binding to vesicles without Chol. Interestingly, their dependence with temperature revealed a different pattern than that of the binding of apoA-I with PC/SM vesicles without cholesterol: the association binding constant (K_a) and the number of lipid molecules per bound protein were no longer constant. Furthermore, the $\Delta H°$ and the $\Delta S°$ no longer exhibited a linear dependence with the temperature. The rationale for that behavior is given in Discussion, below.

Fluorescence microscopy

To examine the characteristics of lipid organization in the membranes, two-photon fluorescence microscopic images were taken at the surface of GUVs of lipid composition that was identical to that of the SUVs. Vesicles were grown at 60°C, labeled with Laurdan (see Methods), and images taken every 7–8° while the temperature decreased to 14°C. A homogeneous bright area was observed at the surface of the GUV at temperatures over ≈37°C, indicating all-liquid surface. Fig. 3 *Aa* shows the image of a POPC/SM GUV at 37.5°C, and Fig. 3 *Ac* displays the image obtained for POPC/SM/Chol GUV at 38.0°C. At lower temperatures, the fluorescence images started showing dark areas in both POPC/SM (Fig. 3 *Ab*) and POPC/SM/Chol (Fig. 3 *Ad*) GUV membranes, corresponding to lo-/ld-phase coexistence. Under these conditions, ld surfaces are POPC-rich domains, whereas more solid areas are SM-rich (See Discussion). The size and shape of the domains remained almost unchanged in the temperature range in which they were observed (15–30°C).

GP *measurements and two-photon fluorescence microscopy*

To characterize the lipid state of the coexisting domains, we determined the *GP* values of the GUVs analyzed previously (Fig. 3 *A*), and *GP* images were taken at the center of the vesicles (Fig. 3 *B*). In agreement with the image of the surface of the vesicles, the *GP* distribution clearly shows two different *GP* areas at low temperatures and just one homogeneous *GP* at the higher temperature tested. The numbers on each image indicate the average *GP* (GP_a) and the *GP* for the two areas with clearly different values (GP_l and GP_s). These values were obtained from the *GP* images using the SimFCS program (Laboratory for Fluorescence Dynamics, Champaign, IL). An interesting observation is that the addition of cholesterol increases the *GP* at the different temperatures tested, and also for each independent domain coexisting at low temperatures. For the liquid-disordered domains, the *GP* changes from −0.19 to −0.05 (ΔGP = 0.14); and for the liquid-ordered domains, the difference is 0.06. It can be deduced that cholesterol partitions within both domains.

ApoA-I binding to GUVs

A binding experiment was performed to detect whether apoA-I will preferentially bind to any of the coexisting lipid domains. Labeled protein was added to GUVs of POPC/SM with and without cholesterol at temperatures below 30°C (Fig. 4, *Aa* and *Ba*, respectively). The GUVs appear slightly ''decorated,'' indicating a weak interaction between the protein and the mixed bilayer. However, under these conditions, the profile of domains delimited later by Prodan was not evident (Fig. 4, *Ab* and *Bb*), indicating that there is probably not a significant preference of apoA-I for binding to different domains of dissimilar composition.

Circular dichroism spectroscopy

Circular dichroism spectroscopy provided the mean number of amino acid residues that are in α-helical conformation in the secondary structure of proteins. This information complements ITC data, since protein conformational changes are normally associated with either release or absorption of heat (45).

CD experiments were carried out for apoA-I in buffer or in the presence of POPC/SM SUVs with or without cholesterol at 15 and 37°C, and the spectra are shown in Fig. 5. Protein/lipid ratio in the CD cuvette was $\sim 15.7 \times 10^{-3}$ w/w for POPC/SM SUVs and 52.6×10^{-3} w/w for POPC/SM/Chol SUVs—i.e., the same at which saturation was reached in the ITC binding experiments, so that protein binding was at maximum in the presence of excess lipid. Table 3 summarizes the experimental data. The fraction of the protein in α-helical conformation was calculated using Eq. 4. A simple calculation based on data in Table 3 and the length of apoA-I at 243 amino acid residues yielded the number of residues that acquired α-helical conformation upon binding to the vesicles.

TABLE 2 Thermodynamic parameters (average of at least three experiments, ±SD) obtained by isothermal titration calorimetry for apoA-I binding to POPC/SM/Chol (molar ratio of 7.5:1.4:1.3) SUVs

T (°C)	N	r	K_a (M^{-1})	$\Delta H°_{prot}$ (kcal/mol)	$\Delta H°_{lipid}$[§] (cal/mol)	$T\Delta S°$(kcal/mol)
15	$(3.5 \pm 0.4) \times 10^{-4}$	1712 ± 119	$(2.2 \pm 0.4) \times 10^{6}$	−69.7 ± 2.8	−41 ± 4	−61.3 ± 1.8
19	$(1.8 \pm 0.2) \times 10^{-4}$	3380 ± 30	$(1.9 \pm 0.3) \times 10^{6}$	−63.7 ± 3.1	−19 ± 2	−55.2 ± 2.2
22	$(1.9 \pm 0.2) \times 10^{-4}$	3133 ± 09	$(12.9 \pm 3.2) \times 10^{6}$	−48.0 ± 2.2	−15 ± 1	−38.3 ± 1.2
25	$(1.6 \pm 0.1) \times 10^{-4}$	3699 ± 06	$(46.4 \pm 9.7) \times 10^{6}$	−32.1 ± 1.6	−9 ± 1	−21.4 ± 0.4

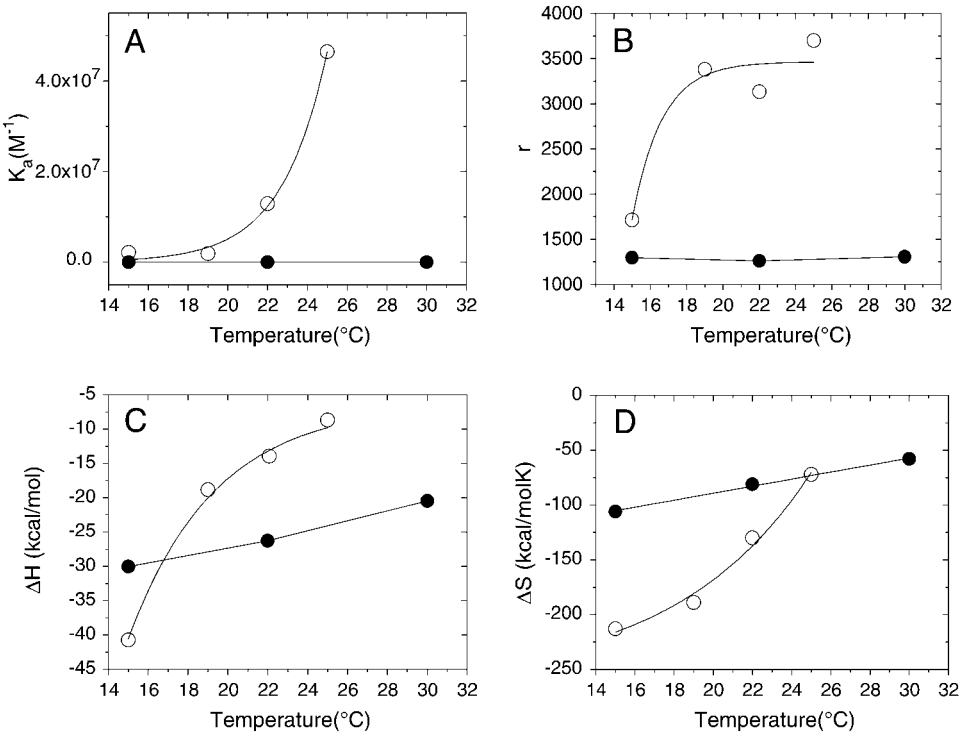

FIGURE 2 Binding of apoA-I to small unilamellar vesicles as a function of temperature. Open circles, POPC/SM/Chol (7.5:1.4:1.3 mol/mol/mol ratio); and solid circles POPC/SM (7.5:1.4 mol/mol ratio). (*A*) Association constant, K_a. (*B*) Number of lipid molecules bound per protein, *r*. (*C*) Enthalpy change, $\Delta H°$. (*D*) Entropy change, $\Delta S°$.

At the physiological temperature of 37°C, 50% of the residues in lipid-free apoA-I were in α-helical conformation, whereas the percentage rose to 82% for apoA-I bound to POPC/SM SUVs. The difference, 32%, was the gain in α-helix content, which corresponded to ~78 residues. In the presence of cholesterol, however, only ~52 residues acquired α-helical conformation. Considering that the latter lipid composition is often considered to be a model for membrane rafts (46,47), this result indicates that raftlike lipid domains would induce a less extensive folding of apoA-I as compared with cholesterol-free model membranes. According to Wieprecht et al. (45), α-helix formation at the surface of SUVs contributes to the enthalpy and entropy change per residue by −0.7 kcal/mol and −1.9 cal/mol K, respectively.

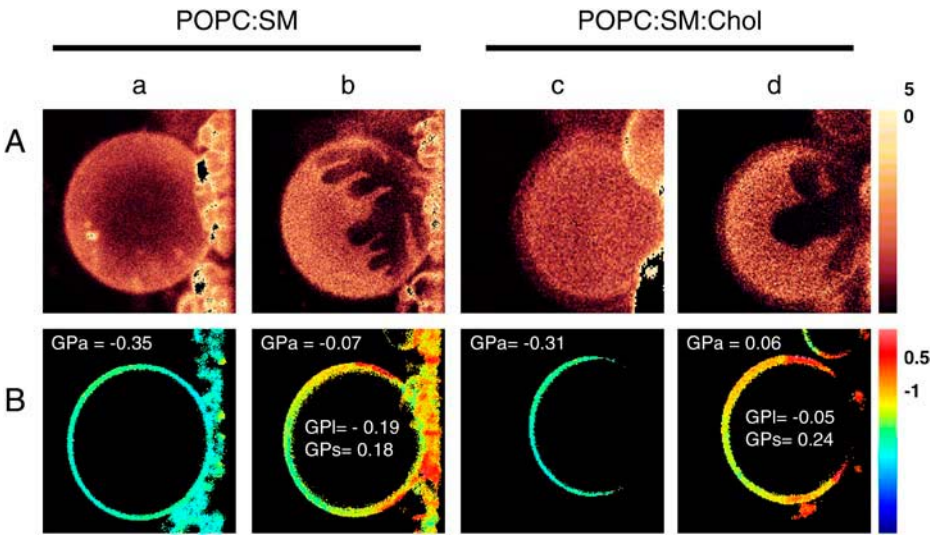

FIGURE 3 Two-photon fluorescence image of Laurdan-doped GUVs containing POPC/SM (7.5:1.4 mol/mol, *a* and *b*) and POPC/SM/Chol (7.5:1.4:1.3 mol/mol/mol, *c* and *d*) at different temperatures. The bright regions on the images showed the lipids in a more fluid state whereas the dark regions corresponded to more tightly packed gel-like lipids. In both mixtures a clear lipid phase separation was observed below 30°C. *A* shows the intensity image from the top of the GUVs of POPC/SM at 38°C (*a*) and at 15°C (*b*) and POPC/SM/Chol at 37.5°C (*c*) and 15.5°C (*d*). The false relative color scale is shown at the right side of the figure (from 0 to 5). *B* shows the *GP* images at the center of the same vesicles. GP_a on the top left of each *GP* image corresponds to the average *GP*. The GP_l and GP_s values correspond to the *GP* for the liquid-disordered (*yellow*) and the liquid-ordered(*red*) areas, respectively. The *GP* values are for this specific GUV; errors in the *GP* values between one GUVs in the same preparation go from 5 to 9%. The false relative color-scale is shown at the right side of the figure (from −1 to 0.5).

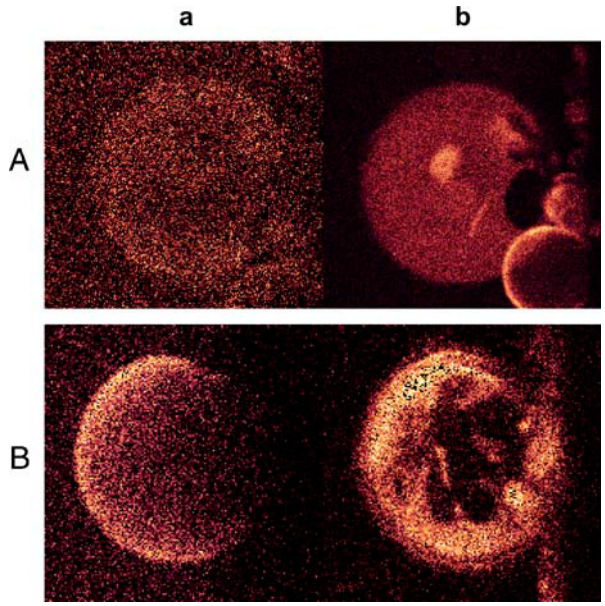

FIGURE 4 Binding of fluorescein-labeled apoA-I to GUVs of POPC/SM at 24°C (*Aa*), and POPC/SM/Chol T 20°C (*Ba*). Panels *Ab* and *Bb* show the same vesicles, respectively, after the addition of Prodan, at the same temperatures.

These values allowed us to estimate the enthalpy and entropy contribution of α-helix formation for apoA-I binding to SUVs.

Comparison of ITC and CD experimental results

The ITC signal is a result of many molecular interactions that take place at the calorimetric cell—namely the properly binding process of apoA-I to lipid vesicles, helix formation, lipid-lipid, and protein-protein interactions as well as hydration effects. To evaluate the partial contribution of processes distinct to helix formation on the enthalpy and entropy changes of the system, we subtracted the contribution of helix formation to $\Delta H°$ and $\Delta S°$ from the values obtained by ITC experiments (Table 4).

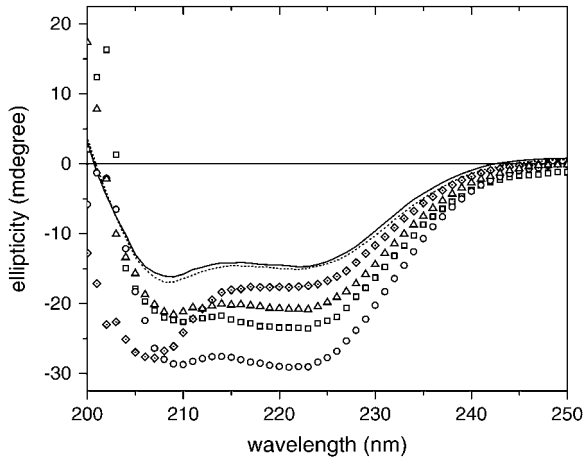

FIGURE 5 Comparative far UV CD spectra of apoA-I in solution and bound to SUVs of different lipid composition, POPC/SM/Chol (7.5:1.4:1.3 mol/mol/mol ratio) and POPC/SM (7.5:1.4 mol/mol ratio). Protein concentration was 3.58 μM for all the incubations tested. At 15°C, TSB (—); POPC/SM/Chol (◇); and POPC/SM (□). At 37°C, TSB (····); POPC/SM/Chol (Δ); and POPC/SM (○).

From Table 4, it is apparent that the folding of apoA-I was the main driving force for the interaction with POPC/SM membranes, whereas other parts of the system contributed positively to $\Delta H°$ (+8.0 kcal/mol) and $T\Delta S°$ (+6.2 kcal/mol), indicating an endothermic disarray during the protein interaction. By the contrary, α-helix formation played a minor role for the binding process of apoA-I to membranes of POPC/SM/Chol. In fact, upon binding to lipid rafts like bilayers, fewer residues acquired α-helical conformation. Our rationale for this behavior is that cholesterol imposes topological constraints to the bilayer, which modify lipid packing and thus hinder the protein insertion into the bilayer, preventing disordering of the lipid matrix. These constraints avoid a deep penetration of apoA-I into the bilayers whose composition mimic that of lipid rafts in biomembranes at the temperatures where the domains are visualized by microscopy.

On the other hand, it has been proposed that hydrophobic interaction of apoA-I with lipid bilayer is favored at the boundaries of lipid domains (48), where two lipid phases coexist. Interestingly, it was recently shown that α-synuclein, a protein present in fibrillar aggregates responsible for a number of neurodegenerative disorders including Parkinson's disease, dementia, and multiple system atrophy has a high affinity for packing defects in a bilayer membrane (49). Similarly, the interaction of apoA-I with the bilayer at higher temperatures, where the lipid domains are melting, could favor the penetration of the apolar side chains into the bilayers, providing additional endothermic contributions to the calorimetric signal, which finally overlap and exceed the exothermic contributions of other events, like the protein folding or van der Waals interactions.

DISCUSSION

The existence of specific lipid domains enriched with cholesterol within the plasma membrane has been proposed to account for the differences in the rate constant for cholesterol desorption from cell membranes. To further investigate this aspect we studied the interaction of apoA-I to model membranes of POPC/SM with or without cholesterol. The present work shows that the lipid-protein binding exhibits analogies and differences when compared to the lipid-protein binding observed for vesicles of pure POPC or of POPC/Chol (18).

Nonclassical hydrophobic interactions

The experimental evidence presented in this study shows that binding of apoA-I to lipid membranes containing SM or SM+Chol cannot be interpreted in terms of classical

TABLE 3 Circular dichroism spectroscopy parameters for the binding of apoA-I to POPC/SM and POPC/SM/Chol SUVs at 15°C and 37°C

	Ellipticity (mdeg)		Number of residues in α-helical structure		Fraction (%)	
	15°C	37°C	15°C	37°C	15°C	37°C
Lipid-free apoA-I	−14.7 ± 0.3	−15.1 ± 0.2	117 ± 2	121 ± 1	48	50
ApoA-I POPC/SM	−21.9 ± 0.4	−23.7 ± 0.7	184 ± 3	199 ± 4	76	82
ApoA-I POPC/SM/Chol	−17.6 ± 0.3	−20.8 ± 0.5	144 ± 3	173 ± 3	59	71

Ellipticity values of apoA-I measured at 222 nm. The corresponding fractions of α-helical structure were determined from Eq. 2.

hydrophobic interaction, but can be in those of the nonclassical hydrophobic reaction, in common with our previous measurements in the absence of SM (18). Molecular interactions dominated by hydrophobic forces are usually driven by entropy rather than enthalpy, characterized by a positive $\Delta S°$, and negative $\Delta C_p°$. In contrast, the nonclassical hydrophobic effect exhibits large exothermic binding enthalpies when sonicated unilamellar vesicles were employed (50). Although interesting, this effect had been observed only on binding of molecules to small, highly curved vesicles and not upon binding to large vesicles. The entropy change is zero or even negative. The negative $\Delta H°$ and the negative $\Delta S°$ could be explained, partly, by the increased van der Waals interactions between lipids or between proteins due to membrane-protein binding. As shown in Table 3, the α-helix content of apoA-I increases with the protein interaction with the bilayers, lowering the dynamics of the amino acid residues involved. Thus helix formation, which is driven by a negative enthalpy change (51), also contributes to the negative entropy of the system.

Effects of SM

Comparison of the thermodynamic data for apoA-I insertion into POPC/SM bilayers in this article with those obtained by Arnulphi et al. (18) for insertion in pure POPC allows us to point out a number of effects attributable to SM. The two sets of data at 30°C are shown together, to facilitate comparison, in Table 5. The two main effects of SM are a large decrease in the enthalpy and entropy changes associated to apoA-I binding, and a change in sign of the heat capacity change, which becomes positive in the presence of SM. As mentioned in Comparison of ITC and CD Experimental Results, above, and Table 4, α-helix formation was the main driving force for apoA-I interaction with POPC/SM bilayers, at 15°C. No CD data are available at 30°C that would permit a direct comparison with the thermodynamic data in Table 5. However, the fraction of protein in α-helical structure was rather constant in the 15–37°C interval for POPC/SM bilayers (see Table 3), and also very similar to the data for pure POPC bilayers at 37°C (18). Thus we can safely assume that the contribution of α-helix formation at 30°C to enthalpy and entropy changes will be very similar to the contribution measured at 15°C (Table 4), and also similar (per mole of bound protein) in POPC and POPC/SM bilayers. If this is the case, then the effect of SM on $\Delta H°$ and $\Delta S°$ is a very large decrease in the contributions of factors other than α-helix formation, i.e., changes in lipid-lipid and lipid-protein interaction, to the enthalpy and entropy changes. SM makes the contributions from the latter factors to change sign, from negative to positive.

The finding that $\Delta C_p°$ for the binding of apoA-I to SM-containing vesicles is positive is interesting, particularly because, when hydrophobic amino acid chains are transferred to the hydrophobic membrane matrix, $\Delta C_p°$ is usually negative (as is indeed the case for apoA-I insertion into pure POPC bilayers; see Table 5). It has been suggested that positive values of $\Delta C_p°$ may arise from conformational (order-disorder) changes in the phospholipid acyl chains (41). In this context, introduction of SM, which is more ordered than POPC and also prone to induce transbilayer interdigitation (52,47), may explain the unusual $\Delta C_p°$.

TABLE 4 Contributions to the enthalpy and entropy changes from factors other than α-helix formation at 15°C

	$\Delta H°$* (kcal/mol)			$T\Delta S°$* (kcal/mol)		
	ITC†	CD‡	Others§	ITC†	CD‡	Others§
POPC/SM	−38.9	−46.9	+8.0	−30.5	−36.7	+6.2
POPC/SM/Chol	−69.7	−18.9	−50.8	−61.3	−14.8	−46.5

*Listed $\Delta H°$ and $T\Delta S°$ values were per mol protein.
†Experimental $\Delta H°$ or $T\Delta S°$ values determined from ITC (see Table 1).
‡Estimated contributions to $\Delta H°$ or $T\Delta S°$ from helix formation (45).
§Contributions to $\Delta H°$ or $T\Delta S°$ from interactions other than helix formation, mainly from lipid-lipid and lipid-protein interactions.

Effects of cholesterol

Because of the uncertainties of thermodynamic measurements of mixtures including SM and Chol at 30°C, data in

TABLE 5 Comparison of the thermodynamic parameters of apoA-I binding to SUV of POPC in the presence and absence of SM, at 30°C

Lipid composition	K_a (M^{-1})	$\Delta H°_{prot}$ (kcal/mol)	$T\Delta S°_{prot}$ (kcal/mol)	n	$\Delta C_p°$ (kcal/K per mol)
Pure POPC*	(4.1 ± 0.9) × 10^6	−101 ± 2	−89 ± 3	3.2	−2.7
POPC/SM (7.5:1.4 mol/mol ratio)†	(3.8 ± 0.4) × 10^6	−27 ± 0.4	−18 ± 0.5	2.3	+0.81

*Data from Ref. 18.
†Data from this article.

the absence and presence of Chol were compared at 15°C (Table 6). Cholesterol reduces slightly the protein-vesicle association constant K_a, and the average number of bound proteins per vesicle n. In turn, it increases by twofold both $\Delta S°$ and $\Delta H°$ of binding. These increments cannot be due, in this case, to an increased α-helix formation, because CD spectroscopy reveals that, in the presence of Chol, less α-helix is actually formed (Table 6). The increased $\Delta H°$ and $\Delta S°$ of binding in the presence of cholesterol must rather be interpreted in terms of increased lipid order, and perhaps formation of SM/Chol complexes (47). The inherently highly ordered, cholesterol-containing bilayer can apparently contribute to a richer network of bonding (more negative $\Delta H°$) upon binding of apoA-I, while reducing protein flexibility (more negative $\Delta S°$), as compared to the situation in the absence of Chol. It is also noteworthy that, in the presence of Chol (Fig. 2), $\Delta H°$ and $\Delta S°$ values increased nonlinearly with temperature, thus an estimation of ΔC_p° was not feasible. This nonlinear behavior is expected when additional processes are coupled in the same reaction (53), such as an ordered-disordered phase transition of the lipid bilayer, or lo-domain disintegration, that, above 30°C, was sensed as an endothermic process, as was measured by ITC in this work.

The influence of lipid domains

Fluorescence microscopy data (Fig. 3) show that, both in the presence and in the absence of Chol, the lipid systems under study undergo lateral phase separation at 15°C. At 38°C, though, the surface bilayer appears homogeneous. This may explain the difficulties in obtaining meaningful thermodynamic data above 30°C, when protein binding is likely to disturb the bilayer phase equilibrium, thus introducing new contributions to the measured heat exchange. The nature of the phase-separation phenomenon at low temperature may be quite different in the presence and absence of the sterol (see Ref. 54). In its absence, lipid mixtures of high-T_m and low-T_m can form coexisting gel and liquid crystalline domains over a temperature range (55), whereas cholesterol promotes lipid phase-separation into lo- and ld-domains (56,57). (Note that T_m is the temperature of the gel-to-liquid crystalline melting transition for a pure lipid.) An interesting result is shown in Fig. 4, in which fluorescence microscopy clearly shows that apoA-I homogeneously binds POPC/SM and POPC/SM/Chol bilayers, under conditions of lateral phase separation, without showing any preference for one particular phase. Thus the phase separation or domain formation is independent from the interaction of apoA-I with the mixed lipid bilayer. Moreover, we have recently analyzed the interactions of apoA-I with phospholipid vesicles showing gel-liquid crystalline lateral coexistence (33). We observed that although lateral separation takes place within a broad range of temperatures, effective lipid solubilization occurs only under very specific temperature conditions where interfacial packing defects are maximal. The results presented here show that, particularly at low temperatures, protein binding may occur in the absence of significant lipid solubilizing activity. Finally, note that GUVs used in the fluorescence microscopy observations differ vastly in size and in radius of curvature from the SUVs used in the calorimetric measurements, so the area of phase boundary is not the same, which can modify the kinetics of the process involved in protein interaction, as was detected by Tricerri et al. (33). For example, protein binding to, as well as lipid solubilization from GUVs were slower than the same processes in sonicated vesicles. No attempt is made in this article to apply in a quantitative way SUV data to GUV observations, or vice versa. Even if thermodynamic studies on GUVs should be interesting, there is not at the moment an accurate procedure to be applied to supported-giant vesicles.

TABLE 6 A comparison of the thermodynamic and structural parameters of apoA-I binding to SUV of POPC/SM in the presence and absence of Chol, at 15°C; data from Tables 1–3

Lipid composition	K_a (M^{-1})	$\Delta H°_{prot}$ (kcal/mol)	$T\Delta S°_{prot}$ (Kcal/mol)	n	% α-helix
POPC/SM (7.5:1.4)	$(3.6 \pm 0.8) \times 10^6$	-39 ± 1.9	-31 ± 1.0	2.3	76
POPC/SM/Chol (7.5:1.4:1.5)	$(2.2 \pm 0.4) \times 10^6$	-70 ± 2.3	-61 ± 1.5	1.7	59

We are very grateful to Prof. F. M. Goñi for the critical reading of the manuscript. The CD and the fluorescence microscopy experiments were performed at the Laboratory for Fluorescence Dynamics at the University of Illinois at Urbana-Champaign.

The Laboratory for Fluorescence Dynamics is supported jointly by the National Center for Research Resources of the National Institutes of Health (PHS 5 P41-RRO3155) and the University of Illinois at Urbana-Champaign. This research was supported by National Institutes of Health grants No. RR-03155 to E.G. and No. HL-16059 to A.J., and Fundación Antorchas grant No. 14022/124 to M.A.T. and C.A.

REFERENCES

1. Francone, O. L., P. V. Subbaiah, A. van Tol, L. Royer, and M. Haghpassand. 2003. Abnormal phospholipid composition impairs HDL biogenesis and maturation in mice lacking ABCA1. *Biochemistry*. 42:8569–8578.
2. Fielding, J. F., and P. E. Fielding. 2001. Cellular cholesterol efflux. *Biochim. Biophys. Acta*. 1533:175–189.
3. Phillips, J. C., W. Wriggers, Z. Li, A. Jonas, and K. Schulten. 1997. Predicting the structure of apolipoprotein A-I in reconstituted high-density lipoprotein disks. *Biophys. J*. 73:2337–2346.
4. Jonas, A., J. H. Wald, K. L. Harms Toohill, E. S. Krul, and K. E. Kezdy. 1990. Apolipoprotein A-I structure and lipid properties in homogeneous, reconstituted spherical and discoidal high density lipoproteins. *J. Biol. Chem*. 265:22123–22129.
5. Jonas, A. 1992. Lipid-binding properties of apolipoproteins. *In* Structure and Function of Apolipoproteins. M. Rosseneu, Boca Raton, FL. 217–250
6. Brewer, H. B. J., T. Fairwell, A. La Rue, R. Ronan, A. Hauser, and T. J. Bronzert. 1978. The amino acid sequence of human APOA-I, an

apolipoprotein isolated from high density lipoproteins. *Biochem. Biophys. Res. Commun.* 80:623–630.

7. Rothblat, G. H., M. de la Llera Moya, V. Atger, G. Kellner-Weibel, D. L. Williams, and M. C. Phillips. 1999. Cell cholesterol efflux: integration of old and new observations provides new insights. *J. Lipid Res.* 40:781–796.

8. Gaus, K., J. J. Gooding, R. T. Dean, L. Kritharides, and W. Jessup. 2001. A kinetic model to evaluate cholesterol efflux from THP-1 macrophages to apolipoprotein A-1. *Biochemistry.* 40:9363–9373.

9. Rietveld, A., and K. Simons. 1998. The differential miscibility of lipids as the basis for the formation of functional membrane rafts. *Biochim. Biophys. Acta.* 1376:467–479.

10. Simons, K., and E. Ikonen. 1997. Functional rafts in cell membranes. *Nature.* 387:569–572.

11. Fielding, C. J., and P. E. Fielding. 2003. Relationship between cholesterol trafficking and signaling in rafts and caveolae. *Biochim. Biophys. Acta.* 1610:219–228.

12. Fielding, C. J. 2001. Caveolae and signaling. *Crit. Opin. Lipidol.* 12:281–287.

13. Brown, D. A. 2001. Seeing is believing: visualization of rafts in model membranes. *Proc. Natl. Acad. Sci. USA.* 98:10517–10518.

14. Edidin, M. 2003. The state of lipid rafts: from model membranes to cells. *Annu. Rev. Biophys. Biomol. Struct.* 32:257–283.

15. Mendez, A. J., G. Lin, D. P. Wade, R. M. Lawn, and J. F. Oram. 2001. Membrane lipid domains distinct from cholesterol/sphingomyelin-rich rafts are involved in the ABCA1-mediated lipid secretory pathway. *J. Biol. Chem.* 276:3158–3166.

16. Bagatolli, L. A., and E. Gratton. 1999. Two-photon fluorescence microscopy observations of shape changes at the phase transition in phospholipid giant unilamellar vesicles. *Biophys. J.* 77:2090–2101.

17. Tricerri, M. A., S. A. Sanchez, C. Arnulphi, D. M. Durbin, E. Gratton, and A. Jonas. 2002. Interaction of apolipoprotein A-I in three different conformations with palmitoyl oleoylphosphatidylcholine vesicles. *J. Lipid Res.* 43:187–197.

18. Arnulphi, C., L. Jin, M. A. Tricerri, and A. Jonas. 2004. Enthalpy-driven apoA-I and lipid bilayer interaction indicating protein penetration upon lipid binding. *Biochemistry.* 43:12258–12264.

19. Leroy, A., and A. Jonas. 1994. Native-like structure and self-association behavior of apolipoprotein A-I in a water/*n*-propanol solution. *Biochim. Biophys. Acta.* 1212:285–294.

20. Breukink, E., P. Ganz, B. de Kruijff, and J. Seelig. 2000. Binding of nisin Z to bilayer vesicles as determined with isothermal titration calorimetry. *Biochemistry.* 39:10247–10254.

21. Wiseman, T., S. Williston, J. F. Brandts, and L. N. Lin. 1989. Rapid measurement of binding constants and heats of binding using a new titration calorimeter. *Anal. Biochem.* 179:131–137.

22. Newman, G. C., and C. Huang. 1975. Structural studies on phosphatidylcholine-cholesterol mixed vesicles. *Biochemistry.* 14:3363–3370.

23. Makhatadze, G. I., and P. L. Privalov. 1990. Heat capacity of proteins. I. Partial molar heat capacity of individual amino acid residues in aqueous solution: hydration effect. *J. Mol. Biol.* 213:375–384.

24. Privalov, P. L., and G. I. Makhatadze. 1990. Heat capacity of proteins. II. Partial molar heat capacity of the unfolded polypeptide chain of proteins: protein unfolding effects. *J. Mol. Biol.* 213:385–391.

25. White, S. H., and W. C. Wimley. 1999. Membrane protein folding and stability: physical principles. *Annu. Rev. Biophys. Biomol. Struct.* 28: 319–365.

26. Parasassi, T., G. De Stasio, G. Ravagnan, R. M. Rush, and E. Gratton. 1991. Quantitation of lipid phases in phospholipid vesicles by the generalized polarization of Laurdan fluorescence. *Biophys. J.* 60:179–189.

27. Angelova, M. I., S. Soleau, P. Meleard, J. F. Faucon, and P. Bothorel. 1992. Preparation of giant vesicles by external fields. Kinetics and application. *Progr. Colloid Polym. Sci.* 89:127–131.

28. Angelova, M. I., and D. S. Dimitrov. 1986. Liposome electroformation. *Faraday Discuss. Chem. Soc.* 81:303–311.

29. Dimitrov, D. S., and M. J. Angelo. 1987. Lipid swelling and liposome formation on solid surfaces in external electric fields. *Prog. Colloid Polym. Sci.* 73:48–56.

30. Bagatolli, L. A., and E. Gratton. 2000. Two photon fluorescence microscopy of coexisting lipid domains in giant unilamellar vesicles of binary phospholipids mixtures. *Biophys. J.* 78:290–305.

31. So, P. T. C., T. French, W. M. Yu, K. M. Berland, C. Y. Dong, and E. Gratton. 1996. Two-photon fluorescence microscopy. *In* Time-Resolved and Intensity Imaging in Fluorescence Imaging Spectroscopy and Microscopy. John Wiley & Sons, New York.

32. So, P. T. C., T. French, W. M. Yu, K. M. Berland, C. Y. Dong, and E. Gratton. 1995. Time-resolved fluorescence microscopy using two-photon excitation. *Bioimaging.* 3:49–63.

33. Tricerri, M. A., J. D. Toledo, S. A. Sanchez, T. L. Hazlett, E. Gratton, A. Jonas, and H. A. Garda. 2005. Visualization and analysis of apolipoprotein A-I interaction with binary phospholipid bilayers. *J. Lipid Res.* 46:669–678.

34. Parasassi, T., E. Gratton, W. Yu, P. Wilson, and M. Levi. 1997. Two photon fluorescence microscopy of Laurdan generalized polarization domains in model and natural membranes. *Biophys. J.* 72: 2413–2429.

35. Eid, J. S., J. D. Muller, and E. Gratton. 2000. Data acquisition card for fluctuation correlation spectroscopy allowing full access to the detected photon sequence. *Rev. Sci. Instrum.* 71:361–368.

36. Tricerri, M. A., A. K. Behling Agree, S. A. Sanchez, J. Bronski, and A. Jonas. 2001. Arrangement of apolipoprotein A-I in reconstituted high-density lipoprotein disks: an alternative model based on fluorescence resonance energy transfer experiments. *Biochemistry.* 40: 5065–5074.

37. Sanchez, S. A., L. A. Bagatolli, E. Gratton, and T. L. Hazlett. 2002. A Two-photon view of an enzyme at work: *Crotalus atrox* venom PLA2 interaction with single-lipid and mixed-lipid giant unilamellar vesicles. *Biophys. J.* 82:2232–2243.

38. Bagatolli, L. A., S. A. Sanchez, T. Hazlett, and E. Gratton. 2003. Giant vesicles, Laurdan, and two-photon fluorescence microscopy: evidence of lipid lateral separation in bilayers. *Methods Enzymol.* 360:481–500.

39. Chen, Y.-H., J. T. Yang, and H. M. Martinez. 1972. Determination of the secondary structures of proteins by circular dichroism and optical rotatory dispersion. *Biochemistry.* 11:4120–4131.

40. Wieprecht, T., M. Beyermann, and J. Seelig. 1999. Binding of antibacterial magainin peptides to electrically neutral membranes: thermodynamics and structure. *Biochemistry.* 38:10377–10387.

41. Spolar, R. S., J. R. Livingstone, and M. T. J. Record. 1992. Use of liquid hydrocarbon and amide transfer data to estimate contributions to thermodynamic functions of protein folding from the removal of nonpolar and polar surface from water. *Biochemistry.* 31:3947–3955.

42. Tsvetkova, N. M., N. J. Walker, A. E. Oliver, L. M. Crowe, J. H. Crowe, and F. Tablin. 1999. Lipid composition and thermal phase transition of human platelet plasma and dense tubular system membranes separated by immunoaffinity. *Mol. Membr. Biol.* 16:265–272.

43. Almeida, R., A. Fedorov, and M. Prieto. 2003. Sphingomyelin/phosphatidylcholine/cholesterol phase diagram. Boundaries and composition of lipid rafts. *Biophys. J.* 85:2406–2416.

44. Heerklotz, H., H. Szadkowska, T. Anderson, and J. Seelig. 2003. The sensitivity of lipid domains to small perturbations demonstrated by the effect of Triton. *Mol. Biol.* 329:793–799.

45. Wieprecht, T., M. Beyermann, and J. Seelig. 2002. Thermodynamics of the coil-α-helix transition of amphipathic peptides in a membrane environment: the role of vesicle curvature. *Biophys. Chem.* 96:191–201.

46. Dietrich, C., L. A. Bagatolli, Z. N. Volovyk, N. L. Thompson, M. Levi, K. Jacobson, and E. Gratton. 2001. Lipid rafts reconstituted in model membranes. *Biophys. J.* 80:1417–1428.

47. Veiga, M. P., J. L. Arrondo, F. M. Goni, A. Alonso, and D. Marsh. 2001. Interaction of cholesterol with sphingomyelin in mixed membranes containing phosphatidylcholine, studied by spin-label ESR and IR spectroscopies. A possible stabilization of gel-phase sphingolipid domains by cholesterol. *Biochemistry.* 40:2614–2622.

48. Swaney, J. J. 1980. Properties of lipid apolipoprotein association products. Complexes of dimyristoyl phosphatidylcholine and human apo A-1. *J. Biol. Chem.* 255:877–881.

49. Nuscher, B., F. Kamp, T. Mehnert, S. Odoy, C. Haass, P. J. Kahle, and K. Beyer. 2004. α-synuclein has a high affinity for packing defects in a bilayer membrane—a thermodynamics study. *J. Biol. Chem.* 279: 21966–21975.

50. Seelig, J., and P. Ganz. 1991. Nonclassical hydrophobic effect in membrane binding equilibria. *Biochemistry.* 30:9354–9359.

51. Massey, J. B., A. M. J. Gotto, and H. J. Pownall. 1979. Contribution of α-helix formation in human plasma apolipoproteins to their enthalpy of association with phospholipids. *J. Biol. Chem.* 254:9359–9561.

52. Veiga, M. P., F. M. Goni, A. Alonso, and D. Marsh. 2000. Mixed membranes of sphingolipids and glycerolipids as studied by spin-label ESR spectroscopy. A search for domain formation. *Biochemistry.* 39:9876–9883.

53. Eftink, M. R., A. C. Anusiem, and R. L. Biltonen. 1983. Enthalpy-entropy compensation and heat capacity changes for protein-ligand interactions: general thermodynamic models and data for the binding of nucleotides to ribonuclease A. *Biochemistry.* 22:3884–3896.

54. London, E., and D. A. Brown. 2000. Insolubility of lipids in Triton X-100: physical origin and relationship to sphingolipid/cholesterol membrane domains (rafts). *Biochim. Biophys. Acta.* 1508:182–195.

55. Lee, A. G. 1977. Lipid phase transitions and phase diagrams. II. Mixtures involving lipids. *Biochim. Biophys. Acta.* 472:285–344.

56. London, E., and G. W. Feigenson. 1981. Fluorescence quenching in model membranes. An analysis of the local phospholipid environments of diphenylhexatriene and gramicidin A′. *Biochim. Biophys. Acta.* 649:89–97.

57. Ahmed, S. N., D. A. Brown, and E. London. 1997. On the origin of sphingolipid/cholesterol-rich detergent-insoluble cell membranes: physiological concentrations of cholesterol and sphingolipid induce formation of a detergent-insoluble, liquid-ordered lipid phase in model membranes. *Biochemistry.* 36:10944–10953.